J. Fluid Mech. (1987), *vol.* 177, *pp.* 109–131
Printed in Great Britain

Measurement of shear-induced self-diffusion in concentrated suspensions of spheres

By DAVID LEIGHTON† AND ANDREAS ACRIVOS
Department of Chemical Engineering, Stanford University, Stanford, CA 94305-5025, USA

(Received 16 August 1985 and in revised form 30 May 1986)

A novel technique is presented for determining the coefficient of shear-induced particle self-diffusion in concentrated suspensions of solid spheres, which relies on the fact that this coefficient can be computed from the measured variations in the time taken by a single marked particle in the suspension to complete successive circuits in a Couette device. Since this method does not involve the direct measurement of the lateral position of the marked particle, it requires a much simpler experiment than that used by Eckstein, Bailey & Shapiro (1977) which is shown to be constrained by wall effects at high particle concentration. The diffusion coefficient thus determined was found to be proportional to the product $\dot{\gamma}a^2$, where $\dot{\gamma}$ is the shear rate and a the particle radius, and to have the asymptotic form $0.5\dot{\gamma}a^2\phi^2$ in the dilute limit when the particle concentration $\phi \to 0$.

1. Introduction

The diffusion of neutrally buoyant small particles in suspensions has received much attention in recent years; however the bulk of the research in this area has been confined to the study of suspensions in which the particles were sufficiently small ($a \lesssim 1$ μm) that particle diffusion was dominated by Brownian motion. In this paper we consider a different source of particle migration, that of shear-induced diffusion, which occurs in suspensions undergoing shear when the motion of the particles due to shear-induced interparticle interactions is much greater than that arising from Brownian motion. We thus confine ourselves to suspensions where the Péclet number ($Pe = \gamma\mu a^3/kT$) is large. This encompasses a wide range of important suspension flows such as the diffusion of red blood cells in arteries.

To understand more fully the phenomenon of shear-induced self-diffusion, consider a single marked particle immersed in a viscous suspension of otherwise identical particles undergoing the simple shear flow $u = \dot{\gamma}y$, where u is the effective fluid velocity in the x-direction and $\dot{\gamma}$ is the shear rate. In the absence of any interparticle interactions, inertial forces, and Brownian-motion effects, the particle will not experience a drift and will simply translate along the streamlines in the flow. When this particle interacts with the other particles in the suspension, however, it will suffer a series of displacements normal to the fluid streamlines which, when taken together, constitute a random walk. Moreover, if the concentration distribution of particles in the suspension is at equilibrium (i.e. uniform for an unbounded linear shear flow), then the particle displacement due to this random walk will have zero mean. Thus,

† Present address: Department of Chemical Engineering, University of Notre Dame, Notre Dame, IN 46556, USA.

since on average the particle will remain on its initial streamline, the process will be akin to classical self-diffusion which, in this case, is shear induced.

It is important to note that the coefficient of self-diffusion associated with this mechanism is not identical with the effective diffusivity which governs the rate of migration of particles along gradients in concentration. This is because, owing in large part to the greater resistance experienced by a particle when moving into regions of higher particle concentration compared to those of lower concentration, its displacement across streamlines will have a non-zero mean in the presence of a gradient in particle concentration, and the particles will experience a net drift from regions of high to low concentration. As a consequence, in the latter case the effective diffusivity will consist of the sum of two terms: one arising from this non-random drift process and the other from the random self-diffusion. In concentrated suspensions of non-uniform composition, this diffusivity is dominated by the drift mechanism (Leighton & Acrivos 1986) since the resistance to particle motion increases rapidly as the particle enters the regions of high concentration. On the other hand, the mixing of labelled spheres in a suspension of uniform solids concentration is entirely controlled by the random self-diffusion process considered here since, owing to the absence of actual gradients in the total concentration of particles, the drift mechanism is also absent.

It is instructive to examine the self-diffusion that arises from purely viscous hydrodynamic interactions between spheres in a suspension. To this end, consider two isolated spheres freely suspended in a Newtonian fluid undergoing a linear shear flow. It is well known that as the two spheres approach each other under these conditions, they become temporarily displaced from their original streamlines, to which they return, however, at the end of the interaction. Since no net displacement has taken place, such interactions cannot lead to diffusion. In the presence of three or more interacting spheres, however, the interaction will, in general, no longer be symmetric and all of the spheres will experience some displacement from their original streamlines, leading to the random walk and self-diffusion described above. In addition, since the rate at which a given sphere interacts with two other spheres simultaneously is proportional to $\dot{\gamma}\phi^2$ as the particle concentration $\phi \rightarrow 0$, and since the length of each step in the random walk is proportional to the particle radius a, we should expect that in a suspension of spheres at low concentrations, the coefficient of self-diffusion should be proportional to $\dot{\gamma}\phi^2 a^2$. It should be noted, however, that in a suspension consisting of anisotropic particles, such as ellipsoids or rods, two-particle interactions are in general not symmetric and hence could lead to finite displacements. One would expect therefore that, for such systems, the coefficient of self-diffusion would be proportional to ϕ, rather than to ϕ^2, in the dilute limit.

It is an interesting consequence of the linearity of the governing flow equations at zero Reynolds number that, in the absence of any non-hydrodynamic forces, the random walks executed by particles in the suspension should be reversible, i.e. the particles should retrace their original paths following a reversal in the direction of flow. As a consequence, under these conditions, the self-diffusion described here constitutes an example of a microscopically reversible diffusion process such as that observed by Okagawa, Ennis & Mason (1978) for the diffusion of the orientation of a dilute suspension of initially uniformly oriented rods undergoing shear in a Couette device. Of course, all such microscopically reversible diffusion processes are very sensitive to any loss of memory, and thus the slight irreversibilities inherent in any physical system, such as non-hydrodynamic surface forces and surface-roughness effects, will quickly render the mixing due to self-diffusion permanent in nature.

The purpose of this paper is to describe an experimental determination of the shear-induced coefficient of self-diffusion of spheres at low Reynolds number by observing the random walk of a marked particle immersed in a suspension undergoing shear in a Couette device. In the next section we examine the only previous attempt at this type of measurement (Eckstein, Bailey & Shapiro 1977) and demonstrate that the data reduction procedure employed there had limitations which resulted in seriously underestimating the diffusion coefficients at the higher particle concentrations that were examined. We then present a new technique which, using only information about the time it takes for a marked particle to complete a circuit about a Couette device, provides an alternative method for evaluating this quantity.

In §3 we describe the implementation of this experimental technique to the measurement of the shear-induced coefficient of self-diffusion of suspensions of spheres as a function of shear rate, particle radius, and concentration. As was expected from the dimensional arguments presented above, this parameter was found to be proportional to the shear rate and to the square of the particle radius, and also proportional to the square of the particle concentration in the dilute limit. The final section contains a summary of our results.

2. Experimental approach

The random migrations of particles in a suspension undergoing shear give rise to a diffusive process which may be characterized in terms of the shear-induced coefficient of self-diffusion. In this section we shall suggest a simple and accurate experimental technique for evaluating this quantity.

2.1. *Basic concepts*

We examine the phenomenon of self-diffusion by investigating the motion of a single marked sphere immersed in a suspension of hydrodynamically identical spheres undergoing the simple shear flow $u = \dot{\gamma} y$. By the ergodic hypothesis, the motion of a single sphere averaged over time may be related to the ensemble-average motion of all of the particles in the suspension. To begin with we need to recall that an isolated particle immersed in a shear field simply translates along the undisturbed streamlines of the flow and hence that v, its instantaneous velocity in the y-direction, will be zero at all times. In a suspension, however, the existence of interparticle interactions leads to non-zero random values of v that cause particle migrations which may, in turn, be related to the diffusion coefficient. Specifically, if we observe the location of the particle in the y-direction after each of $N+1$ intervals in time, we may define a quantity D_{obs}:

$$D_{\text{obs}} = \frac{1}{2N} \sum_{i=1}^{N} \frac{\Delta y_i^2}{\Delta t_i}, \tag{2.1}$$

with Δy_i^2 denoting the square of the increment Δy_i, whose expectation value (i.e. its average value after many experiments) will be shown presently to approach the diffusion coefficient D as

$$\left\langle \frac{1}{\Delta t_i} \right\rangle \equiv \frac{1}{N} \sum_{i=1}^{N} \frac{1}{\Delta t_i} \to 0. \tag{2.2}$$

To determine the relationship between the observed and the actual diffusion coefficients, we begin by considering the particle motion in the y-direction. We have that

$$\Delta y(t) = \int_0^t v(t_1)\, \mathrm{d}t_1, \tag{2.3}$$

and

$$\Delta y^2(t) = \int_0^t \int_0^t v(t_1)\, v(t_2)\, \mathrm{d}t_1\, \mathrm{d}t_2, \tag{2.4}$$

where $\Delta y^2(t)$ denotes the square of the change in $y(t)$. Hence, taking the expectation value (ensemble average) of Δy^2, we obtain the integral

$$\langle \Delta y^2(t) \rangle = \int_0^t \int_0^t \langle v(t_1)\, v(t_2) \rangle\, \mathrm{d}t_1\, \mathrm{d}t_2. \tag{2.5}$$

The relationship between diffusion and migrations in the y-direction is complicated by periodic motions of the marked particle in addition to the truly diffusive random walks. For example, in a dilute suspension, periodic motions may arise from two-sphere interactions, as mentioned in §1. Recall that during such an interaction each sphere is displaced from its initial streamline, to which, however, it returns when the interaction has been completed. Clearly, although no net migration or diffusion has taken place, $\langle \Delta y^2 \rangle \neq 0$ for this encounter. In more concentrated suspensions such two-sphere interactions are rare; however, in this case the particles tend to form aggregates which rotate in the shear field (Graham & Bird 1984; Graham & Steele 1984) and thereby induce a second source of periodic motion. The contribution of periodic motions to the observed diffusion coefficient may be estimated if we assume that the instantaneous velocity v of the particle is the sum of periodic and random terms, i.e.

$$v = v'(t) + v_{\mathrm{p}}(t), \tag{2.6}$$

where $v'(t)$ is a random function with zero mean and $v_{\mathrm{p}}(t)$ is the periodic motion.

We thus obtain for the integrand of (2.5)

$$\langle v(t_1)\, v(t_2) \rangle = \langle v_{\mathrm{p}}(t_1)\, v_{\mathrm{p}}(t_2) \rangle + \langle v_{\mathrm{p}}(t_1)\, v'(t_2) \rangle + \langle v'(t_1)\, v_{\mathrm{p}}(t_2) \rangle + \langle v'(t_1)\, v'(t_2) \rangle. \tag{2.7}$$

The last term in (2.7) is simply $R(\tau)$, the autocorrelation function for the random motion, where $\tau = t_1 - t_2$. This function has a maximum at $\tau = 0$ and decreases rapidly as τ increases at a rate which depends on the source of the random motion. In the case under consideration here, particle migration is caused by shear-induced interparticle interactions; thus $R(\tau)$ should vanish at the end of each interaction. The timescale for such interactions is inversely proportional to the shear rate $\dot{\gamma}$; thus $R(\tau) \to 0$ for $\tau \gg 1/\dot{\gamma}$.

Since the second and third terms of (2.7) vanish because of the assumed randomness of $v'(t)$, we obtain

$$\langle \Delta y^2(t) \rangle = \int_0^t \int_0^t R(t_1 - t_2)\, \mathrm{d}t_1\, \mathrm{d}t_2 + \int_0^t \int_0^t \langle v_{\mathrm{p}}(t_1)\, v_{\mathrm{p}}(t_2) \rangle\, \mathrm{d}t_1\, \mathrm{d}t_2, \tag{2.8}$$

which may be rewritten as

$$\langle \Delta y^2(t) \rangle = 2 \int_0^t (t - \tau)\, R(\tau)\, \mathrm{d}\tau + \int_0^t \int_0^t \langle v_{\mathrm{p}}(t_1)\, v_{\mathrm{p}}(t_2) \rangle\, \mathrm{d}t_1\, \mathrm{d}t_2. \tag{2.9}$$

If, moreover, $t \gg 1/\dot{\gamma}$, then we may extend the upper limit of the first integral to $t = \infty$ and replace the second integral by the expectation value $\langle \Delta y_{\mathrm{p}}^2 \rangle$ for the periodic motion. Thus

$$\langle \Delta y^2(t) \rangle \approx 2t \int_0^\infty R(\tau)\, \mathrm{d}\tau - 2 \int_0^\infty \tau R(\tau)\, \mathrm{d}\tau + \langle \Delta y_{\mathrm{p}}^2 \rangle. \tag{2.10}$$

In an actual experiment some error will always be associated with the observation

of the position of the particle. If we assume that this sighting error is random with some variance $\langle \Delta y_{\text{sight}}^2 \rangle$ then we may write

$$\langle \Delta y_{\text{obs}}^2 \rangle = \langle \Delta y^2 \rangle + \langle \Delta y_{\text{sight}}^2 \rangle. \tag{2.11}$$

Finally, combining (2.1), (2.10) and (2.11), and making use of the identity between the integral of the autocorrelation function $R(\tau)$ and D,

$$D \equiv \int_0^\infty R(\tau)\, \mathrm{d}\tau, \tag{2.12}$$

we obtain for the expectation value of D_{obs}

$$\langle D_{\text{obs}} \rangle = D + \frac{1}{t}\left(\langle \Delta y_{\text{sight}}^2 \rangle + \langle \Delta y_{\text{p}}^2 \rangle - 2 \int_0^\infty \tau R(\tau)\, \mathrm{d}\tau \right). \tag{2.13}$$

Thus the difference between the observed and actual diffusion coefficients may be reduced by increasing t, the length of time between successive observations, since the contribution to $\langle \Delta y^2 \rangle$ due to both the observation errors and the periodic motion do not grow with time.

2.2. *Previous experimental work*

The approach outlined above for calculating the diffusion coefficient is precisely that employed by Eckstein *et al.* (1977). These authors carried out their measurements in a Couette device of major radius $R = 6$ in. and gap width $W = 1.053$ in. A single radioactively labelled particle was placed in a suspension of otherwise identical particles and its radial position (the y-direction in the shear field) and the elapsed time since the previous sighting were determined each time it passed an observation window. To reduce the contribution to the calculated diffusion coefficient arising from the periodic motions and the observation errors, successive transits were combined, thereby effectively increasing the time Δt_i and the migration length Δy_i used in (2.1) to obtain D_{obs}.

The most critical assumption in the derivation of (2.13) was that the shear field was unbounded. We now consider the implications of this assumption. In an infinite shear field no constraints are placed on the motion of the migrating particle in the y-direction. Indeed, after a very long period of time and as a consequence of its random walk, this particle would have been expected to have wandered over great distances in the y-direction. In a Couette device, of course, the existence of the walls constrains such a migration and, as a consequence, limits the maximum diffusion coefficient that may be calculated correctly using (2.1). In fact, for larger values of D the migrations will be wall limited and the use of (2.1) will underestimate the actual diffusion coefficient. Specifically, in order to utilize (2.1) we must require that the diffusion length (given by $(2D\Delta t)^{\frac{1}{2}}$) of a particle migration be much less than the distance between the centre and the walls of the device. Thus

$$\frac{(2D\Delta t)^{\frac{1}{2}}}{\frac{1}{2}W} \ll 1. \tag{2.14}$$

Now, if the particle moves with the velocity of the midpoint of the channel, then the time between observations Δt will be given approximately by

$$\Delta t = \frac{2\pi n R}{u} = \frac{2\pi n R}{\dot{\gamma}\frac{1}{2}W}, \tag{2.15}$$

where $2\pi R$ is the circumference of the Couette device and n is the number of successive observations that have been summed together, the product $2\pi nR$ thus equalling the total path length of the marked particle in the x-direction. Moreover, since from dimensional analysis we anticipate that the shear-induced diffusion coefficient will be proportional to the shear rate and the square of the particle radius (i.e. $\hat{D} = D/\dot{\gamma}a^2$), we may rewrite (2.14) using (2.15) as

$$4\left(\hat{D}\frac{2\pi a^2 nR}{W^3}\right)^{\frac{1}{2}} \ll 1. \tag{2.16}$$

The condition given in (2.16) places a constraint on the maximum dimensionless diffusion coefficient that can be measured using a specific particle size and experimental apparatus. To reduce the effects of wall limitations in their calculations, Eckstein *et al.* (1977) rejected all data except those for which migrations began in the central fifth of the Couette gap. They then required that this region be at least two diffusion lengths from the wall. If the diffusion length based on the calculated diffusion coefficient satisfied this condition, then D_{obs} was assumed to be free of wall limitations. Unfortunately, as is demonstrated in detail in the Appendix, it is possible to show from the data available in Eckstein's thesis (1975) that this condition was not sufficiently stringent and that, for large $\hat{D}$, their experiment appears to have been wall limited, leading to a reported diffusion coefficient that was much less than the correct value. For sufficiently small values of $\hat{D}$, however, it is likely that wall limitation was avoided and that their reported values are correct.

In order to calculate the diffusion coefficient using (2.1), we must not only detect the marked particle, but also accurately measure its position in the narrow gap. Thus, the greatest difficulty in implementing the method used by Eckstein *et al.* (1977) to measure the diffusion coefficient arises from the fact that it is almost impossible to select a particle small enough to avoid wall limitations and yet still large enough for its position to be accurately measured. This suggests the desirability of formulating some alternative to (2.1) for calculating the diffusion coefficient which does not entail the measurement of the position of the particle within the gap. In the next section we do this by developing a relationship between the diffusion coefficient and variations in the times taken for a marked particle to complete successive transits of the Couette device.

2.3. *Determination of diffusion coefficients from transit times*

We begin our analysis by again considering the case of a single marked particle immersed in an infinite suspension undergoing simple shear flow. We wish to relate variations in the time it takes for the particle to travel a distance x_0 (equivalent to $2\pi nR$ in a Couette device) to migrations in the y-direction and hence to the diffusion coefficient in that direction. Clearly, since the velocity of the particle is a function of its position in the y-direction, any lateral migrations also lead to variations in the length of time taken by the particle to complete one circuit. To explicitly determine this relationship, we make use of the transition probability density $P(x, y|t, 0, \xi)$ which is the probability density of the sphere being found at (x, y) at some time t given that it was released at $(0, \xi)$ at $t = 0$. This function is equal to the concentration distribution of a dye diffusing in the same shear flow which results from an initial distribution $\delta(x)\,\delta(y-\xi)$, and satisfies the convective diffusion equation:

$$\frac{\partial P}{\partial t} + \dot{\gamma}y\frac{\partial P}{\partial x} - D\left(\frac{\partial^2 P}{\partial x^2} + \frac{\partial^2 P}{\partial y^2}\right) = 0, \tag{2.17}$$

where we have assigned equal values to the diffusion coefficient in the x- and y-directions. Although the analysis may easily be extended to the case of unequal diffusivities, this will prove unnecessary since we shall demonstrate that diffusion in the x-direction is negligible. In writing (2.17) we have also assumed a homogeneous medium throughout the flow field, i.e. a constant shear rate and constant particle concentration, and have neglected all periodic motions of the particle.

For a Couette device, the appropriate boundary conditions for (2.17) should be zero flux at $y = 0$ and $y = W$ since the particle must be confined to this region; however, in keeping with our assumption of an infinite shear field (and also in order to obtain a closed-form solution) we shall apply the alternate condition that P vanishes at infinity. This should prove adequate provided that during the course of its migrations the particle remains far from the walls. We thus obtain the well-known (see, for example, Frankel & Acrivos 1968) self-similar solution:

$$P(x, y \mid t, 0, \xi) = \frac{1}{2\pi\sigma_y \sigma_x} \exp\left[-\frac{(y-\xi)^2}{2\sigma_y^2}\right] \exp\left[-\frac{(x-\frac{1}{2}\dot{\gamma}t\,(y+\xi))^2}{2\sigma_x^2}\right], \tag{2.18}$$

where

$$\sigma_y^2 = 2Dt, \quad \sigma_x^2 = \tfrac{1}{6}(\dot{\gamma}t)^2\, Dt + 2Dt. \tag{2.19}$$

The two terms in σ_x^2 give the relative magnitude of convection and diffusion in the x-direction, whose ratio

$$\frac{\text{diffusion}}{\text{convection}} = \frac{2Dt}{\frac{1}{6}(\dot{\gamma}t)^2\, Dt} = \frac{12}{(\dot{\gamma}t)^2} = \frac{3W^2}{n(2\pi R)^2} \tag{2.20}$$

is likely to be very small for any experimental device (the ratio has a value of about 2×10^{-3} for the apparatus used by Eckstein 1975). Thus we shall neglect diffusion in the x-direction and let

$$\sigma_x^2 = \tfrac{1}{6}(\dot{\gamma}t)^2\, Dt. \tag{2.21}$$

We may now use the function $P(x, y \mid t, 0, \xi)$ to develop the relationship between the diffusion coefficient in the y-direction and the difference between successive transit times. Let t be the first transit time, defined as the time for which $x = x_0$, and t' be the second transit time. The particle thus undergoes the two successive migrations:

$$(0, 0, \xi) \rightarrow (t, x_0, y) \rightarrow (t + t', 2x_0, y').$$

We wish to obtain $p(t' \mid t)$, the probability density of completing the second transit of the device in time t' given that the first transit was completed in time t. We may determine $p(t' \mid t)$ in terms of several other probability density functions. The first of these is $p'(y \mid t)$ which we define as the probability that a particle which has completed the transit $x = x_0$ in time t is at the lateral position y. This probability density can be calculated as follows.

The joint probability density of the marked particle being at the point (x, y) after a time t, provided that its lateral position ξ at the start of the migration is unknown, is given by

$$p(x, y \mid t) = \int_{-\infty}^{\infty} P(x, y \mid t, 0, \xi)\, p(\xi)\, \mathrm{d}\xi, \tag{2.22}$$

where $P(x, y \mid t, 0, \xi)$ is given by (2.18) and $p(\xi)$ is the probability density that the particle began the transit at $(0, \xi)$. The latter is, in general, a function of the experimental equipment. In a Couette device we are observing the migration of the particle from a fixed position (the observation window), thus, since the velocity of

the suspending fluid is proportional to ξ, the flux of spheres passing the observation point will be greatest near the outer wall. The probability density of observing the marked particle at ξ is therefore proportional to the particle flux at ξ, thus

$$p(\xi) = \begin{cases} 0, & \xi < 0, \xi > W, \\ \dfrac{2\xi}{W^2}, & 0 < \xi < W. \end{cases} \tag{2.23}$$

Using the joint probability distribution $p(x, y \mid t)$ given in (2.22), it is then a simple matter to calculate the probability density over y:

$$p'(y \mid t) = \frac{p(x_0, y \mid t)}{\int_{-\infty}^{\infty} p(x_0, y \mid t)\, \mathrm{d}y}, \tag{2.24}$$

which is normalized over y since the particle must exit at some lateral position.

In order to obtain a closed-form expression for $p(x, y \mid t)$ in (2.22) and for $p'(y \mid t)$ in (2.24), we shall assume that $p(\xi) = 2\xi/W^2$ for all values of ξ, rather than just in the interval $0 < \xi < W$ as in (2.23). But, since the integrand of (2.22), $P(x, y \mid t, 0, \xi)\, p(\xi)$, vanishes exponentially for ξ sufficiently different from y, this will be acceptable provided that the marked sphere is located several diffusion lengths away from the walls of the device. This is the same assumption originally made in deriving (2.18), and thus represents a consistent approximation. Consequently, using the expression for $P(x, y \mid t, 0, \xi)$ given in (2.18), we may now evaluate (2.22) and (2.24) to obtain, approximately,

$$p'(y \mid t) \approx \frac{1}{2}\left(3 - y\frac{\dot{\gamma}t}{x_0}\right)\frac{\sqrt{3}}{(2\pi)^{\frac{1}{2}}\sigma_y} \exp\left[\frac{-3}{2\sigma_y^2}\left(y - \frac{x_0}{\dot{\gamma}t}\right)^2\right], \tag{2.25}$$

which, for small σ_y, approximates a Gaussian distribution about the expected value $y = x_0/\dot{\gamma}t$. The function is skewed toward $y < x_0/\dot{\gamma}t$ since $p(\xi)$ is not constant.

The second probability density function that we require is $p''(t' \mid y)$, the probability density over t' of completing the second transit of the device in time t' given that the second migration began at a lateral position y. To begin with, we note that the cumulative probability of the particle completing the second transit during time t' is given by

$$\mathscr{P}(t', y) = 1 - \int_{-\infty}^{x_0} \int_{-\infty}^{\infty} P(x', y' \mid t', 0, y)\, \mathrm{d}y'\, \mathrm{d}x', \tag{2.26}$$

which is simply one minus the probability of the particle remaining in the region $-\infty < x' < x_0$; thus, the probability density that the particle would have exited from this region during the period $[t', t' + \mathrm{d}t']$ is

$$p''(t' \mid y) = \frac{\partial}{\partial t'}\mathscr{P}(t', y), \tag{2.27}$$

which may be evaluated to yield

$$p''(t' \mid y) = \left(\frac{3}{2}\frac{x_0}{\dot{\gamma}t'} - \frac{1}{2}y\right)\frac{\dot{\gamma}}{(2\pi)^{\frac{1}{2}}}\frac{1}{2\sigma_{x'}} \exp\left[-\frac{(x_0 - \dot{\gamma}t'y)^2}{8\sigma_{x'}^2}\right], \tag{2.28}$$

where $\sigma_{x'}^2 = \frac{1}{6}(\dot{\gamma}t')^2 Dt'$. Again, for small $\sigma_{x'}$, this function approaches a Gaussian distribution about the expected value $t' = x_0/\dot{\gamma}y$.

The desired probability density $p(t' \mid t)$ is therefore the product of $p''(t' \mid y)$ and $p'(y \mid t)$, integrated over all possible values of y, i.e.

$$p(t' \mid t) = \int_{-\infty}^{\infty} p''(t' \mid y) p'(y \mid t) \, dy, \tag{2.29}$$

which may be evaluated to yield

$$p(t' \mid t) = \frac{1}{(2\pi)^{\frac{1}{2}}} \left(\frac{3}{2D(t+t')} \right)^{\frac{1}{2}} \frac{1}{4} \frac{x_0}{\dot{\gamma} t'^2} \times \left[\frac{(2t^2+3tt'-t'^2)(2t'^2+3tt'-t^2)}{tt'(t+t')^2} + \frac{2}{3} \frac{Dt^2t'^2}{(t+t')} \left(\frac{\dot{\gamma}}{x_0} \right)^2 \right] \times \exp\left[\frac{-(t'-t)^2}{\frac{4}{3}Dt^2t'^2(t+t')(\dot{\gamma}/x_0)^2} \right], \tag{2.30}$$

and which relates the diffusion coefficient in the y-direction to variations in the observed transit times t and t'. Note that for small values of the diffusion coefficient, (2.30) simply states that the difference between successive transit times approximates a Gaussian distribution with a variance that is proportional to the diffusion coefficient and the fifth power of the transit time.

In the derivation of (2.30) we have assumed that during the course of its random migrations, the particle will remain far from the walls of the experimental device. For a Couette device, this condition is equivalent to requiring that, during the course of the migration, the distance between the average position of the particle and the walls of the device be much greater than the characteristic diffusion length of the migration. But since in our experiments no direct measurement is made of the particle position, it is necessary to recast this condition into one involving the transit time. Let us require, then, that the probability of the particle encountering the walls at the end of the second migration (i.e. $y'' < 0$ or $y'' > W$) be less than 0.005, given that the first transit was completed in time t. For small values of the diffusion coefficient, the probability distribution for y'' is approximately Gaussian with mean $x_0/\dot{\gamma}t$ and standard deviation $(\frac{8}{3}Dt)^{\frac{1}{2}}$. Thus, the condition imposed above is equivalent to requiring that the mean position be at least three standard deviations from the walls, which should limit the error arising from wall effects to less than 1 %. The condition on t arising from the inner wall is then given by

$$24 \frac{Dt}{(x_0/\dot{\gamma}t)^2} < 1, \tag{2.31}$$

and that from the outer wall is

$$\frac{24Dt}{(W-x_0/\dot{\gamma}t)^2} < 1. \tag{2.32}$$

Consequently, for a fixed experimental geometry, these conditions place an upper bound on the diffusion coefficient which can be measured without introducing errors due to wall limitations.

An examination of the exponential part of $p(t' \mid t)$ reveals that the expression may be recast into a simpler form if we rewrite it as a probability density over a new variable α, defined as

$$\alpha^2 = \frac{(t'-t)^2}{\frac{1}{3}t^2t'^2(t+t')(\dot{\gamma}/x_0)^2}. \tag{2.33}$$

In view of (2.30), the probability density $p^*(\alpha \mid t)$ is therefore given by

$$p^*(\alpha \mid t) \equiv \frac{\partial t'}{\partial \alpha} p(t' \mid t) = \frac{1}{(2\pi)^{\frac{1}{2}}} \frac{1}{(2D)^{\frac{1}{2}}} \exp\left[\frac{-\alpha^2}{4D}\right] \times \left[1 + \frac{1}{2}\frac{t(t'-t)}{t'(t+t')} + \frac{1}{3}\frac{Dt^3t'}{2t^2+3tt'-t'^2}\left(\frac{\dot{\gamma}}{x_0}\right)^2\right], \quad (2.34)$$

which can be simplified further by recognizing that, for small D, the function is exponentially small except near $\alpha = 0$. Thus, expanding (2.33) and (2.34) for small α we have

$$t' = t\left[1 + \left(\frac{2}{3}\frac{\dot{\gamma}^2t^3}{x_0^2}\right)^{\frac{1}{2}}\alpha + \frac{5}{4}\left(\frac{2}{3}\frac{\dot{\gamma}^2t^3}{x_0^2}\right)\alpha^2 + O\left(\left(\frac{2}{3}\frac{\dot{\gamma}^2t^3}{x_0^2}\right)^{\frac{3}{2}}\alpha^3\right)\right] \quad (2.35)$$

and

$$p^*(\alpha \mid t) = \frac{1}{2\pi}\frac{1}{(2D)^{\frac{1}{2}}} \exp\left[-\frac{\alpha^2}{4D}\right]\left[1 + \frac{1}{4}\left(\frac{2}{3}\frac{\dot{\gamma}^2t^3}{x_0^2}\right)^{\frac{1}{2}}\alpha - \frac{1}{8}\left(\frac{2}{3}\frac{\dot{\gamma}^2t^3}{x_0^2}\right)\alpha^2 + O\left(\left(\frac{2}{3}\frac{\dot{\gamma}^2t^3}{x_0^2}\right)^{\frac{3}{2}}\alpha^3\right) + \frac{1}{12}Dt\left(\frac{\dot{\gamma}t}{x_0}\right)^2\left(1 + O\left(\left(\frac{2}{3}\frac{\dot{\gamma}^2t^3}{x_0^2}\right)^{\frac{1}{2}}\alpha\right)\right)\right], \quad (2.36)$$

which, for small values of the diffusion coefficient, approaches a Gaussian distribution with zero mean and variance $2D$, independent of the first transit time t. Using this expression for $p^*(\alpha \mid t)$, we have then for the variance of α:

$$\langle \alpha^2 \rangle|_t = \int_{-\infty}^{\infty} \alpha^2 p^*(\alpha \mid t)\, d\alpha,$$

$$= 2D\left(1 - \frac{5}{12}\left(\frac{\dot{\gamma}t}{x_0}\right)^2 Dt + O\left(\left(\frac{\dot{\gamma}t}{x_0}\right)^2 Dt\right)^2\right), \quad (2.37)$$

which, on substituting the constraint given in (2.31), approaches $2D$, with a maximum deviation from this value of less than 2 %.

We conclude, therefore, that it is possible to calculate the shear-induced coefficient of self-diffusion by making use of successive measurements of the time it takes a marked particle to complete a circuit of a Couette device. Thus, if we observe a series of $N+1$ transit times t_i, we find from (2.37) that the diffusion coefficient will be given approximately by

$$\left.\begin{aligned} D_{\text{obs}} &\approx \frac{1}{2N}\sum_{i=1}^{N} \alpha_i^2, \\ \text{where} \qquad \alpha_i^2 &= \frac{(t_i - t_{i-1})^2}{\frac{1}{3}t_i^2 t_{i-1}^2 (t_i + t_{i+1})(\dot{\gamma}/x_0)^2}, \end{aligned}\right\} \quad (2.38)$$

and where the conditions (2.31) and (2.32) on the first transit time must be satisfied to ensure that the migrations are not wall limited.

The determination of the diffusion coefficient through the use of (2.38) is potentially much more accurate than through (2.1) which requires the direct measurement of the position of the particle in the gap. This improvement in accuracy arises from two sources. First, for a particular absolute observation error, the relative error in the measured transit time $\Delta t_{\text{error}}/\Delta t$ will be much less than the corresponding error in the lateral position $\Delta y_{\text{error}}/\Delta y$, because the circumference of the Couette device is

much greater than the gap width. The ratio of these two relative errors is approximately equal to the ratio of the circumference to the gap width which, for the device used by Eckstein (1975), results in a reduction in error of nearly two orders of magnitude.

Secondly, the existence of periodic (non-random) motions is less important to migrations in the x-direction (and hence to transit times) than to lateral migrations. This is because, although the total contribution of periodic motion to migrations in both the x- and y-directions may be the same, random migrations in the x-direction, which result from random lateral migrations to faster or slower moving streamlines, are amplified by the convection term $\dot{\gamma}t$ while periodic migrations in the y-direction are not. As a consequence, the contribution of periodic motion to the observed diffusion coefficient calculated using (2.38) will again be less than that using (2.1) by a factor $2\pi R/W$, rendering this source of error negligible as well.

In any real Couette device the calculation of the diffusion coefficient using (2.38) is complicated by the fact that the device posseses finite curvature. Indeed, in the device used by Eckstein (1975) the ratio W/R was about $\frac{1}{6}$, which is non-negligible. As a consequence, both the local shear rate (to which the shear-induced diffusion coefficient is proportional) and the path length for a complete transit of the device will be functions of the radial position in the gap. If the diffusion coefficient is small, however, then the variation in the particle position during a migration will also be small and both $\dot{\gamma}$ and x_0 may be treated as effectively constant for each migration. The error in this approximation will be $O((\frac{1}{3}D\bar{t})^{\frac{1}{2}}/R)$ which, for the device used by Eckstein (1975) and the condition on D given by (2.30), is less than 1 %.

If we further assume the flow in the gap to be Newtonian (a good approximation at low particle concentrations) then it is a simple matter to relate the observed transit times to the average position of the particle in the gap during each migration and hence to effective values of $\dot{\gamma}$ and x_0. We thus obtain

$$\left.\begin{aligned} \dot{\gamma}_{\text{eff}} &= \frac{4\pi\nu}{\epsilon}\left(1-\frac{n\epsilon}{\nu\bar{t}}\right), \\ (x_0)_{\text{eff}} &= 2\pi nR\left(1-\frac{n\epsilon}{\nu\bar{t}}\right)^{-\frac{1}{2}}, \end{aligned}\right\} \tag{2.39}$$

where ϵ is given by

$$\epsilon = \frac{W}{R}\left(2+\frac{W}{R}\right)\Big/\left(1+\frac{W}{R}\right)^2,$$

$\bar{t}$ is the average of the two successive transit times t and t', R is the radius of the inner wall of the Couette device, and ν is the frequency of rotation of the outer wall of the Couette device. In terms of these variables we can define an effective value of α:

$$\alpha^2_{\text{eff}} = \frac{(t'-t)^2}{\frac{1}{3}a^2\dot{\gamma}_{\text{eff}}\,t^2t'^2(t+t')\,(\dot{\gamma}/x_0)^2_{\text{eff}}}, \tag{2.40}$$

whose variance is equal to the dimensionless diffusion coefficient $2\hat{D}$ to within a few percent.

It should be noted that since the dimensionless diffusion coefficient calculated from experimental data by means of (2.40) is proportional to $\dot{\gamma}^{-3}$, rather than to $\dot{\gamma}^{-1}$ as in the technique employed by Eckstein *et al.* (1977), it will be much more sensitive to errors in the estimate of the shear rate, such as those resulting from the existence of wall slip regions. Karnis, Goldsmith & Mason (1966) provide observations of the velocity distribution in Couette flow as a function of particle size and concentration,

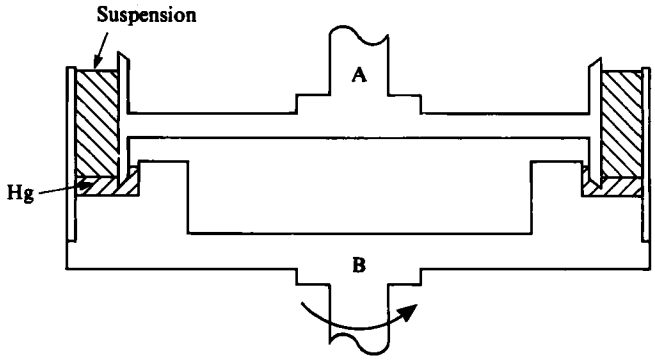

FIGURE 1. The Couette device: A, bob; B, cup. The suspension is confined in the annular region between bob and cup, supported by a layer of mercury.

however, and from these measurements we may conclude that, for an experimental geometry such as that used by Eckstein (and also that employed in our experimentation), particles that are sufficiently small to avoid wall limitations will also be small enough that the deviation from Newtonian flow in the gap is negligible.

3. Experimental work

In this section we present the details of our measurements of the shear induced coefficient of self-diffusion. The basic approach consisted of measuring the successive times taken by a single marked sphere, immersed in a suspension of otherwise identical particles, to complete a circuit of a Couette device. Once this information was obtained, the shear-induced diffusion coefficient was calculated from (2.38) and (2.40).

3.1. *Materials*

The detection apparatus used by Eckstein and his co-workers consisted of a radioactively labelled particle and a radiation detector which was capable of not only detecting the marked particle as it passed an observation window, but also of measuring its position within the gap. In our work, however, a simpler apparatus was employed since the data reduction method developed here obviated the need to directly measure the position of the particle within the gap. Thus, the particle was detected optically: a single opaque sphere was immersed in a suspension of transparent, but otherwise identical, spheres, and the index of refraction of the suspending fluid was matched to that of the transparent spheres, enabling us to see the marked particle. A stopwatch was employed to measure the time taken by the particle to complete each circuit of the device, as determined by its successive crossings of a line marked on the stationary inner cylinder.

The suspension containing the marked particle was placed in the Couette device depicted in figure 1. The radius of the inner wall of the device (the Couette bob) was 9.73 cm and the outer wall (the Couette cup) was 11.74 cm, yielding a gap width of 2.01 cm. The height of the fluid in the gap varied, depending on the total quantity of fluid placed in the gap, but was typically about 4 cm. Since an optical detection technique was employed, the outer wall of the Couette device was constructed of Plexiglas and was mounted on an aluminum base. The large eccentricity inherent in the commercially available acrylic ring used for this outer wall was greatly reduced

by machining the ring in its mounting to a tolerance of ± 50 μm. The inner wall was machined from an aluminum block and was circular to within ± 25 μm. The Couette device was mounted on a model R-17 Weissenberg Rheogoniometer obtained from Sangamo Transducers, Inc. Both the bob and cup of the Couette device were accurately aligned with the axis of rotation of the cup.

The solids used in our experiment consisted of two fractions that were sieved from a single lot of 600 μm mean diameter acrylic particles, obtained from ICI, which were approximately spherical. Only a small fraction of these were fused or otherwise eccentric. The particles were also observed to contain bubbles of varying size, which led to some polydispersity in the density. To reduce the degree of polydispersity, the fraction containing the larger spheres was density segregated in an aqueous potassium iodide solution of density 1.18 g/cm^3. The fraction of spheres that sank in this fluid was collected and dried. These particles were found to have an average density of 1.178 g/cm^3 and an optically determined average size of 645 μm plus a size distribution characterized by the standard deviation ± 46 μm. Unfortunately, the quantity of the smaller spheres collected through sieving was insufficient to permit any density segregation, nor was their density measured; however, since they came from the same lot as the larger spheres, their density was assumed to be similar. This was later verified from the very small rise velocity exhibited by the particles when immersed in the pure fluid whose density matched that of the 645 μm density segregated spheres. The small spheres had an optically determined size distribution of 389 ± 22 μm.

The suspending fluid in all experiments consisted of a solution composed of 40.67 % glycerin, 22.82 % ethylene glycol, and 36.51 % styrene glycol by weight. Since styrene glycol is a solid at room temperature (22 °C), the solution was prepared at 70 °C in a stoppered flask and then cooled. The solution has a viscosity of 2.8 P and exhibited no shear thickening or thinning behaviour over the range of shear rates used in our experiments. It was, however, supersaturated at room temperature in that, after several days, the styrene glycol formed visible crystals (about 1 mm in size) in a suspension at rest. Also, in the presence of shear the rate of crystallization was significantly higher so that crystals appeared during the course of our measurements. This rapid crystallization was attributed to the increase in fluid mixing due to the interaction of the spheres in the sheared suspension.

The density and the index of refraction of the solution were matched to those of the acrylic spheres. Since the index of refraction of the fluid matched that of the acrylic, spheres that did not contain bubbles could be seen only in outline whereas the bubbles present in other particles showed up clearly. When suspensions at particle concentrations below 20 % were sheared in the Couette device, they were observed to stratify somewhat, the particles without bubbles concentrating near the bottom and the more buoyant ones migrating to the top. From this we see that the pure-fluid density was within the narrow range of densities of the 645 μm spheres. At higher concentrations the suspension appeared to be well mixed at the shear rates used in our experimentation.

Two marked particles were used in the experiments, one taken from each size fraction. These were prepared by spray painting a quantity of spheres from both fractions with orange enamel spray paint, and then selecting one from each lot that had a size comparable to the average size of each fraction. The thin coat of enamel did not appear to affect the density of the marked particles, in that they showed no tendency to migrate to the top or bottom of a sheared suspension, but only seemed to add to their surface roughness which it was hoped was not significant enough to

influence their diffusion. The optically measured sizes of the two particles were 645 μm and 421 μm, respectively.

To conduct the experiments, the Couette bob was lowered into the cup until the two were nearly in contact, as is depicted in figure 1. Five pounds of mercury were then poured into the base of the device and the resulting layer, approximately 1 cm in depth, provided an essentially stress-free lower boundary to the suspension. The aluminum base plate was brushed with a small quantity of glycerin prior to the addition of the mercury in order to protect it from the latter. A known quantity of the pure fluid was then poured into the gap, followed by the addition of unmarked acrylic spheres until the desired concentration was attained. The marked sphere was inserted and the suspension was thoroughly mixed, first with a spatula and then by shearing in the Couette device for a total length of strain of about 4000. The measurements were begun once the suspension appeared to have reached equilibrium.

3.2. *Results*

In order to ensure that any observed migrations of the marked particle in the suspension were due only to diffusive migrations, it was necessary to rule out the existence of any significant secondary currents in the Couette gap. Their presence would have increased the observed diffusion coefficient by increasing the magnitude of the migrations in the y-direction which, in turn, would have affected the observed transit times. The strength of these possible secondary currents were determined by examining the behaviour of an isolated particle in the Couette device. The 645 μm marked sphere was immersed in the pure suspending fluid in the Couette gap and sheared at shear rates from 1.5 s^{-1} to 6 s^{-1}. The drift of the particle in the radial (y) direction could then be determined from variations in the time that the particle took to complete a transit of the device. When the particle was placed at the midpoint of the upper half of the channel, it drifted toward the inner wall in such a way that the transit time changed by about 0.6 % during each transit. Conversely, when placed at the midpoint of the lower half of the channel, the particle migrated toward the outer wall with approximately the same magnitude of velocity. The drift velocity did not seem to be affected by variations in the shear rate over the range covered by our experiments, nor was it possible to determine the cause of the secondary currents; however, they were sufficiently small so as not to affect the observed diffusion coefficient, at least at the higher suspension concentrations investigated. For example, a suspension of 645 μm spheres at 30 % concentration exhibited a characteristic fluctuation in transit time of about 10 %, well above the 0.6 % observed for the secondary currents. In more dilute suspensions, however, the magnitude of the diffusive migrations became smaller, and thus for these systems the marked particle was carefully placed near the centre of the device where the secondary currents appeared to be smallest.

The diffusion-coefficient experiments were conducted at solids concentrations ranging from 4.6 to 40 % for the 645 μm acrylic spheres and 15 to 25 % for the 389 μm spheres. In all cases the data consisted of a series of observed successive transit times which could be combined using (2.38) and (2.40) to obtain the diffusion coefficient. Pairs of transit times were used in the calculations only if the first transit time was such that the average position of the particle during the first transit was in the central third of the Couette gap. In order to reduce the contribution of particle sighting errors and of periodic motions, the successive transit times were summed in the data reduction procedure, i.e. the time taken to complete n circuits of the device was used rather than the time to complete a single transit. The benefit of this, discussed in

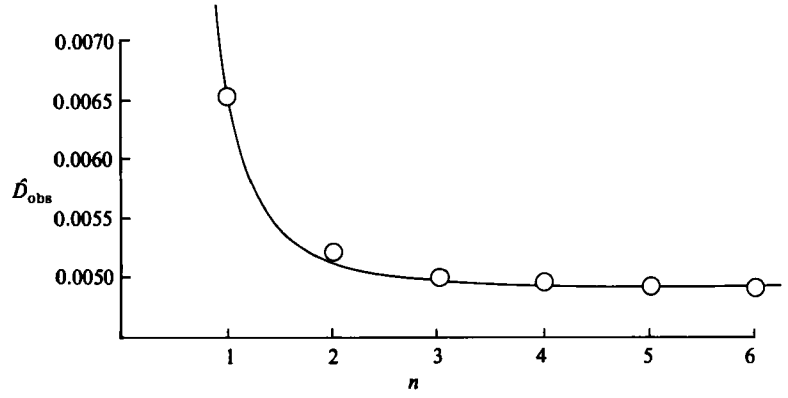

FIGURE 2. Calculated diffusion coefficient *vs.* the number of successive transits summed. Data for 645 μm spheres, 10% concentration, $\dot{\gamma} = 3\ s^{-1}$. The curve is given by $\hat{D}_{obs} = 0.0049 + 0.0016\, n^{-3}$ which corresponds to an observation error of $\sigma_{obs} \approx \pm 0.10$ s.

§2.3, was especially apparent at the lowest concentrations where the magnitudes of the sighting errors and of the diffusive migrations for a single transit were comparable. This may be seen graphically in figure 2 where we have plotted the calculated diffusion coefficient $\hat{D}_{obs}$ versus the number n of transits summed in the data reduction scheme for a suspension of 645 μm spheres at 10% solids concentration. Note that when the transits were taken singly, a very high diffusion coefficient was calculated which decreased rapidly to a lower asymptotic value as the number of jumps summed increased. In this case, the diffusion coefficient was sufficiently small that the migrations were not wall limited even after summing six transits. The fact that the calculated diffusion coefficient in figure 2 approached an asymptotic value with an increase in the number of transits summed shows that, in the absence of wall limitations, the mean-square variation in the transit time is proportional to the average of the fifth power of the transit time, i.e. $\langle \Delta t^2 \rangle \sim \langle t^5 \rangle$ for large t. Moreover, since variations in the transit time result from variations in the velocity of the particle which, in turn, is a function only of its radial position within the gap, the existence of a finite asymptote demonstrates that the mean-spare displacement of the particle in the radial direction grows linearly with time, and that the observed phenomenon is indeed a diffusion process.

We may also use the data presented in figure 2 to estimate the magnitude of our experimental error in the observation of transit times. Thus, if we assume that each observation of the particle has associated with it an error with variance σ^2_{obs} which may arise both from purely observational errors as well as from any particle motion that is not associated with actual migration, such as a periodic motion, then we may estimate the influence of this error on the calculated diffusion coefficient. Specifically, for small values of the diffusion coefficient, the difference between successive transit times is much less than the transit times themselves. As a consequence, the primary contribution to the error in the variable α_i used in calculating the diffusion coefficient from (2.38) will result from errors in the measurement of this difference. Thus, the variance of α_i will be given approximately by

$$\sigma^2_{\alpha_i} \approx \frac{6\sigma^2_{obs}}{\frac{1}{3}t_i^2\, t_{i-1}^2 (t_i + t_{i-1})\, (\dot{\gamma}/x_0)^2}. \tag{3.1}$$

Next, if we let $\alpha_i = \alpha_i^{(t)} + \alpha_i^{(error)}$ where $\alpha_i^{(t)}$ is the contribution to α_i from the actual

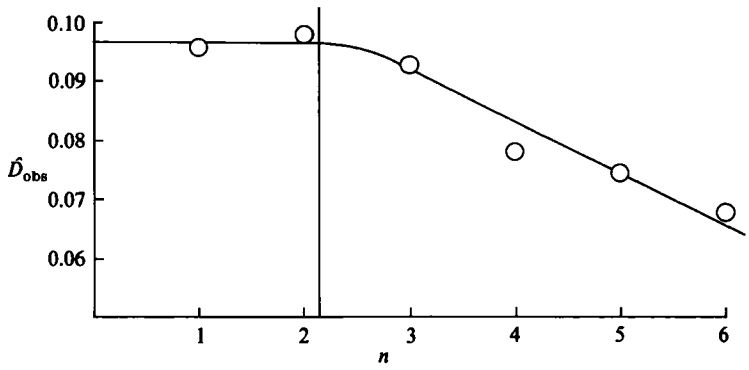

FIGURE 3. Calculated diffusion coefficient *vs.* the number of successive transits summed. Data for 645 μm spheres, 28.1 % concentration, $\dot{\gamma} = 6\ \mathrm{s}^{-1}$.

random migration of the marked particle, and further define, by analogy with (2.38), the diffusion coefficient arising from this motion as

$$D^{(t)} = \frac{1}{2N} \sum_{i=1}^{N} (\alpha_i^{(t)})^2, \tag{3.2}$$

then, for large N, we obtain

$$D_{obs} \approx D^{(t)} + \left\langle \frac{3\sigma_{obs}^2}{\frac{1}{3}t_i^2 t_{i-1}^2 (t_1 + t_{i-1})(\dot{\gamma}/x_0)^2} \right\rangle. \tag{3.3}$$

Moreover, if the particle is located, on average, in the centre of the channel, then the characteristic transit time will be $t_i \approx 2W/\dot{\gamma}x_0$ and, since for our Couette device $x_0 = n2\pi R$, (3.3) reduces in dimensionless form to

$$\hat{D}_{obs} = \hat{D}^{(t)} + \left[\frac{9}{512\pi^3} \frac{\dot{\gamma}^2 W^5}{R^3 a^2}\right] \frac{\sigma_{obs}^2}{n^3}, \tag{3.4}$$

where $\hat{D}_{obs} = D_{obs}/\dot{\gamma}a^2$ and $\hat{D}^{(t)} = D^{(t)}/\dot{\gamma}a^2$. We thus expect that the value of the diffusion coefficient calculated from a given set of data should approach an asymptotic value as n^{-3} for an increasing number of transits n summed in the calculation, provided, of course, that the data are not wall limited. Examination of the data presented in figure 2 confirms this expectation and yields an estimate of the observational error of about ± 0.1 s.

A markedly different behaviour is depicted in figure 3 which presents the data for a 28.1 % suspension of 645 μm spheres. In this case the observed diffusion coefficient was much greater; thus the calculated value, at least initially, did not change greatly as n increased. For $n \geqslant 3$, however, the calculated diffusion coefficient was found to decrease, a behaviour that was attributed to the onset of wall limitation. The point at which the restrictions imposed by (2.31) and (2.32) were exceeded is given by the vertical line in figure 3, which lies ahead of the region where the observed diffusion coefficient is seen to drop off. The best estimate of the actual diffusion coefficient was therefore taken to be the observed value that was obtained from summing the largest possible number of transits without violating (2.31) and (2.32).

In addition to the error, given in (2.13), that arises from using finite transit times, the diffusion coefficient is also subject to a statistical error, analogous to that computed for any variance, due to the finite number of available observations. This error is governed by the chi-square probability distribution; however, for a large

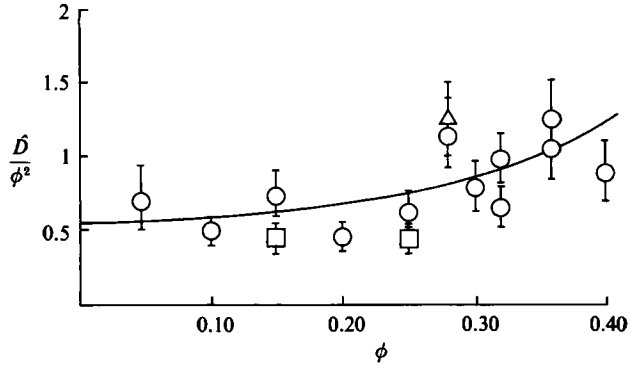

FIGURE 4. Observed coefficient of self-diffusion. Note that $\hat{D}$ is plotted in the form $\hat{D}/\phi^2$. ○, $a = 323$ μm, $\dot{\gamma} = 3\ \mathrm{s}^{-1}$; △, $a = 323$ μm, $\dot{\gamma} = 6\ \mathrm{s}^{-1}$; □, $a = 195$ μm, $\dot{\gamma} = 3\ \mathrm{s}^{-1}$. Curve is best fit to data, $\hat{D} = 0.5\phi^2\,(1 + 0.09\,\mathrm{e}^{7\phi})$.

number of observations, the distribution of observed values of the diffusion coefficient should approach the Gaussian form where the one standard-deviation error in the calculated value is given approximately by

$$\sigma_D \approx D\left(\frac{2}{N}\right)^{\frac{1}{2}}, \tag{3.5}$$

where N is the number of observations.

Using the procedure outlined above, we have found the shear-induced coefficient of self-diffusion to be proportional to $\dot{\gamma}a^2$, as was expected from dimensional arguments, and to be approximately proportional to the square of the particle concentration ϕ for dilute suspensions and to increase somewhat more rapidly than that at higher ϕ. A plot of the experimentally determined diffusion coefficients is given in figure 4, together with the 2σ error bars arising from the statistical source described by (3.5). The number of transit times used in the experiments varied, but typically approximately 200 observations were used in each calculation.

At this stage it is instructive to compare the diffusion coefficients measured in this work with those obtained by Eckstein *et al.* (1977). As may be seen from figure 5, our observations are in good agreement with theirs for concentrations up to 20 %. Beyond this, however, the diffusion coefficients measured in this work continue to grow rapidly (our measurements at concentrations above 32 % are off-scale in this figure), whereas Eckstein *et al.*'s approach a constant value. The discrepancy suggests that, as will be discussed in more detail in the Appendix, the diffusion coefficients observed by Eckstein *et al.* (1977) at high concentrations were limited by the presence of the walls.

The greatest experimental difficulty that we encountered was in maintaining a uniform concentration throughout the Couette gap. This arose because of the polydisperse density of the particles, which caused the particles without bubbles to sink and those with a greater buoyancy to float. The problem was especially severe at lower concentrations where the diffusion coefficient was also small since diffusion, of course, would have tended to render the suspension more homogeneous. As a consequence, although every effort was made to mix the suspensions as thoroughly as possible and to place the marked particle carefully, the concentration corresponding to the observed diffusion coefficients was undoubtedly subject to considerable measurement error.

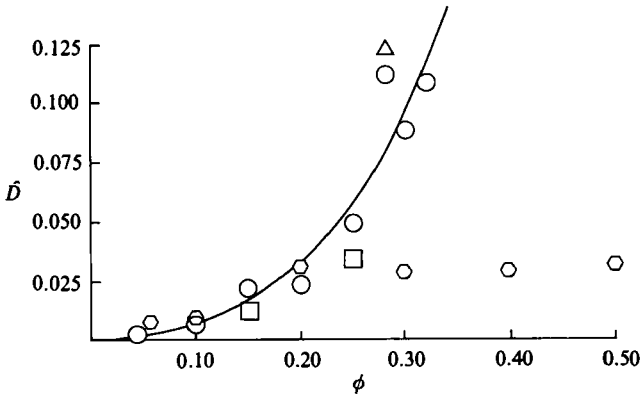

FIGURE 5. Comparison of the diffusion coefficient measured in this paper with that observed by Eckstein *et al.* (1977). Measured in this work: ○, $a = 323$ μm, $\dot{\gamma} = 3\ s^{-1}$; △, $a = 323$ μm, $\dot{\gamma} = 6\ s^{-1}$; □, $a = 195$ μm, $\dot{\gamma} = 3\ s^{-1}$. Measured by Eckstein *et al.*: ⬡, $a = 1600$ μm; $\dot{\gamma} = 10\ s^{-1}$ (data taken from Eckstein *et al.* (1977), figure 2). Solid curve is best fit to experimental data $\hat{D} = 0.5\phi^2\ (1 + 0.09\ e^{7\phi})$.

A second source of difficulty arose from the crystallization of the styrene glycol from the suspending fluid during the course of the experiments. Since this occurred only gradually as the suspension was sheared, it was absent from the early stages of the experiments and only became visible toward the end. Separately, viscosity measurements on suspensions with $\phi = 0.40$ showed that crystallization influenced the effective viscosity only after approximately 100 minutes of shearing at $\dot{\gamma} = 2.4\ s^{-1}$, which implies that the diffusion measurements were probably unaffected up to that point since the viscosity is a more rapidly increasing function of ϕ than is D. Besides, as no differences were detected between the diffusion coefficients measured before and after the onset of crystallization, it appears unlikely that this phenomenon significantly affected our observations. Further experimentation is necessary to resolve this issue, however.

4. Summary

In this paper we have developed a relationship between the shear-induced coefficient of self-diffusion parallel to gradients in fluid velocity and variations in the time it takes for a marked particle immersed in the suspension to complete a circuit of a Couette device. Since this only requires that we measure the transit time of a marked particle in a Couette device and obviates the need of also determining the particle position within the Couette gap, it greatly simplifies the experimental apparatus required by Eckstein *et al.* (1977). The technique was employed to measure the coefficient of self-diffusion in suspensions of 645 μm and 389 μm acrylic spheres as a function of concentration and shear rate.

The diffusion coefficient was found to be proportional to the shear rate and the square of the particle radius and to be an increasing function of concentration ϕ, approximately equal to $0.5\ \phi^2$ at low concentrations. This is in contrast to the linear dependence of the diffusion coefficient on concentration that was reported for dilute suspensions by Eckstein *et al.* (1977). The result arrived at here is, however, more in accordance with what would have been expected at low Reynolds numbers since, in the absence of non-hydrodynamic contact forces (which should be absent in dilute

suspensions), at least three interacting spheres are required for any permanent displacement of the particles to occur; hence, we conclude that the dilute-limit diffusion coefficient should be proportional to ϕ^2 as was observed in our experiments.

The coefficient of self-diffusion at high concentrations ($\phi > 30\,\%$) measured here, while greater than those reported by Eckstein *et al.* (1977), are still much less than the effective diffusion coefficient measured using a different approach (Leighton & Acrivos 1986). This is as would be expected since, as was described in §1, the effective diffusion coefficient is the sum of both random and non-random drift components of which the latter was shown (Leighton & Acrivos 1986) to increase very rapidly with concentration – approximately in proportion to $(\phi^2/\mu_r)(\mathrm{d}\mu_r/\mathrm{d}\phi)$ where μ_r is the relative viscosity of the suspension. Hence, this component would be expected to dominate self-diffusion at high ϕ since the coefficient of self-diffusion was observed to grow only slightly more rapidly than ϕ^2 at concentrations above 30 %.

Although the experimentally determined values of the diffusion coefficient exhibited a considerable degree of scatter, they appear to be approximately correct and demonstrate the efficacy of using Couette transit times for this purpose.

This work was supported in part by the Department of Energy, under grant nos. 80-ER10659 and 85-ER13328, by the National Science Foundation under grant no. CPE 81-17299, by a National Science Foundation fellowship for D.T.L. and by Nato Research grant no. 538.83.

Appendix. Analysis of the diffusion-coefficient measurement technique due to Eckstein, Bailey & Shapiro (1977)

In his dissertation work, Eckstein (1975) developed a technique for measuring the shear-induced coefficient of self-diffusion of a suspension of neutrally buoyant spherical particles in a linear shear field. His apparatus consisted of a concentric cylinder Couette device with a gap width $W = 1.053$ in. and a major radius $R = 6$ in. A single radioactively labelled sphere was placed in a slurry of otherwise identical spheres and its radial position was determined by a radiation detector. Since the detector was fixed in place whereas the outer cylinder rotated, the labelled sphere would be observed once each time it passed the detector. Thus the data that were obtained from this device consisted of a series of times between successive observations of the particle and the associated change in the radial position. For such data, it is possible to calculate the observed value of the diffusion coefficient D_{obs}:

$$D_{\mathrm{obs}} = \frac{1}{2N}\sum_{i=1}^{N}\frac{\Delta y_i^2}{\Delta t_i}, \tag{2.1}$$

which, as was described in §2, will approach the asymptotic value of the diffusion coefficient D as

$$\left\langle\frac{1}{\Delta t}\right\rangle = \frac{1}{N}\sum_{i=1}^{N}\frac{1}{\Delta t_i}$$

becomes small provided that the migrations in the radial direction are not limited by the presence of the walls. The relationship between D_{obs} and D under this assumption is given by

$$D_{\mathrm{obs}} = D + \tfrac{1}{2}\langle\Delta y_{\mathrm{error}}^2\rangle\left\langle\frac{1}{\Delta t}\right\rangle, \tag{A 1}$$

where $\langle \Delta y^2_{\text{error}} \rangle$ is some average value of the increase in the observed variance over that due to strictly random migrations. A discussion of the sources of this error term was also given in §2. In this Appendix we shall examine in detail Eckstein's data reduction technique and, using data available in his thesis (Eckstein 1975), shall show that it seriously underestimated the values of the diffusion coefficient at the high concentrations, owing to wall limitations.

Experimentally, Eckstein attempted to minimize the difference between D_{obs} and D by summing successive jumps until the combined Δt for the composite jump was greater than some chosen value $\Delta t_{\min}$. These composite jumps were then used in conjunction with (2.1) to calculate a value of the diffusion coefficient. In order the evaluate Eckstein's reduction procedure, we require knowledge of the average value $\langle 1/\Delta t \rangle$ that corresponds to a particular choice of $\Delta t_{\min}$. Without the experimental data it is impossible to determine this relationship exactly except, of course, that the average of the inverse transit times is less than the inverse of the minimum transit time. We shall estimate the deviation of $\langle 1/\Delta t \rangle$ from $1/\Delta t_{\min}$ as follows.

A particle whose average position during the course of its migration is in the central region of the Couette gap will complete a circuit of the device in a time $\bar{t} = 4\pi R/\dot{\gamma} W$ equal to the circumference divided by the mid-channel velocity. After a sufficiently long period of time has elapsed from the initial observation (at $t = 0$) the probability of detecting the particle in a time interval $t < \Delta t < t + \mathrm{d}t$ will become independent of t, i.e. the position of the particle in the gap in the direction of motion will become random. Moreover, if the particle moves with a velocity such that it completes a circuit of the device in time $\bar{t}$, then the probability density of first observing a particle at time t after a time $\Delta t_{\min}$ has passed is approximately given by

$$p(t) \approx \begin{cases} 1/\bar{t}, & \Delta t_{\min} < t < \Delta t_{\min} + \bar{t}, \\ 0, & t > \Delta t_{\min} + \bar{t}. \end{cases} \tag{A 2}$$

Thus, we may write

$$\left\langle \frac{1}{\Delta t} \right\rangle \approx \int_{\Delta t_{\min}}^{\Delta t_{\min}+\bar{t}} \frac{1}{\bar{t}} \frac{\mathrm{d}t}{t} = \frac{1}{\bar{t}} \ln\left(1 + \frac{\bar{t}}{\Delta t_{\min}}\right) \tag{A 3}$$

as an estimate for $\langle 1/\Delta t \rangle$ which approaches the value of $1/\Delta t_{\min}$ when $\Delta t_{\min}/\bar{t} \gg 1$.

We shall now use (A 1) and the estimated value of $\langle 1/\Delta t \rangle$ to examine the calculated diffusion coefficient as a function of $\Delta t_{\min}$ given by Eckstein (1975) in his figure (6.4) and reproduced here (figure 6). In this figure the diffusion coefficient (solid diamonds) is plotted versus the minimum time interval used in its calculation from a shear rate $\dot{\gamma} = 10\ \text{s}^{-1}$, sphere radius $a = \frac{1}{16}$ in., and suspension concentration $\phi = 40\,\%$. Under these conditions the expected particle transit time $\bar{t}$ is approximately 7.2 s. The first experimental point given by Eckstein is for $\Delta t_{\min} = 4$ s. The probability of the labelled sphere having completed a circuit of the device in less than this time is very low for the shear rate used, thus we shall take $\langle 1/\Delta t \rangle = 1/\bar{t} = 1/7.2\ \text{s}^{-1}$ for this case. All other values of $\langle 1/\Delta t \rangle$ are estimated using (A 3). We may thus reduce the data of figure 6 to the tabular form given in table 1, and then fit them by a linear regression to (A 1) to obtain an estimate of the actual diffusion coefficient and the magnitude of the error. We thus obtain

$$D_{\text{obs}} = 0.0010 + 0.11 \left\langle \frac{1}{\Delta t} \right\rangle \text{cm}^2/\text{s}, \tag{A 4}$$

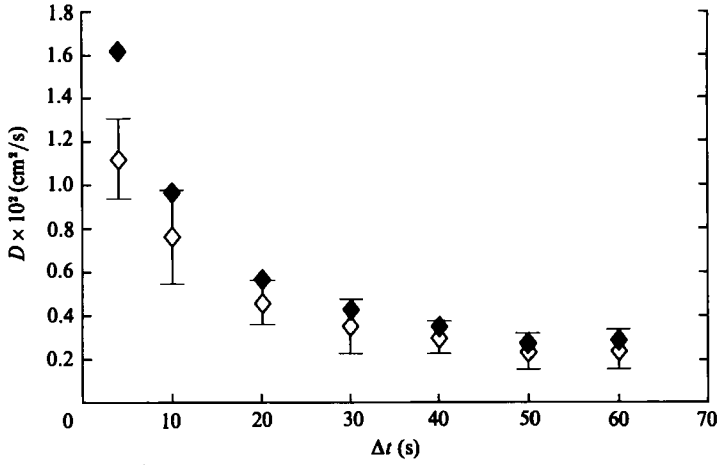

FIGURE 6. Observed diffusion coefficient as a function of $\Delta t_{\min}$. Reproduced from Eckstein (1975, figure 6.4). ◆, diffusion coefficient; ◇, diffusion coefficient corrected using (A 1) and $\langle \Delta y^2_{\text{error}} \rangle$.

$\Delta t_{\min}$ (s)	4	10	20	30	40	50	60
$\langle 1/\Delta t_i \rangle$ (s^{-1})	0.14	0.075	0.043	0.030	0.023	0.019	0.016
D_{obs} (cm²/s)	0.0162	0.0098	0.0057	0.0043	0.0035	0.0028	0.0028

TABLE 1. Diffusion coefficients observed by Eckstein (1975) and estimated value of $\langle 1/\Delta t_i \rangle$ in his experiments as a function of $\Delta t_{\min}$.

with a correlation coefficient $\rho = 0.999$. Or, in dimensionless terms

$$\hat{D}_{\text{obs}} = D_{\text{obs}}/\dot{\gamma}a^2 = 0.0040 + 0.44\left\langle \frac{1}{\Delta t_i} \right\rangle, \tag{A 5}$$

where the fact that the correlation coefficient ρ is so close to unity indicates that (A 5) provides a very good fit to the data.

Eckstein (1975) chose a value of $\Delta t_{\min} = 20$ s for the reduction of his data and, therefore, reported $\hat{D}_{\text{obs}} = 0.023$ for this experiment. From the analysis given above, however, it appears that this choice of $\Delta t_{\min}$ was incorrect since, if the system were not wall limited, a corrected value of $\hat{D} = 4 \times 10^{-3}$ would have been calculated instead from (A 5). The latter is nearly an order of magnitude below that reported by Eckstein (1975) and very close to zero given their experimental error. In addition, from the fit of the data to (A 1), we find that the estimated error $\langle \Delta y^2_{\text{error}} \rangle$ is very large, approximately $4.4a^2$, i.e. more than an order of magnitude greater than that estimated by Eckstein.

Using (A 1) and his estimated value of $\langle \Delta y^2_{\text{error}} \rangle$, Eckstein calculated a corrected value of the diffusion coefficient, which is given by the open diamonds in figure 6. But based on the analysis leading to (A 1), we would expect that if his estimate of $\langle \Delta y^2_{\text{error}} \rangle$ were accurate, then his corrected values would be independent of $\Delta t_{\min}$, which clearly they are not. It must be concluded, therefore, that either the sources of error in Eckstein's experiment were much greater than he estimated, and hence that the actual diffusion coefficient was much lower than reported, or the assumption

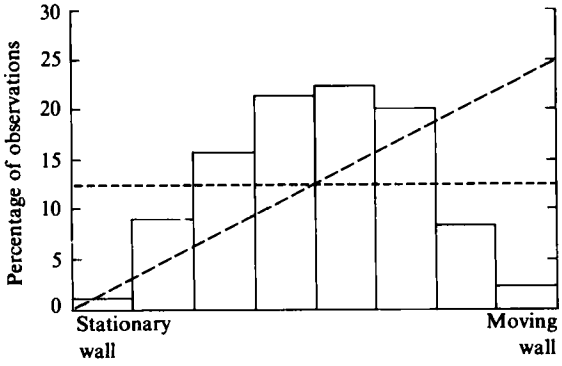

FIGURE 7. Distribution of particle sightings. Reproduced from Eckstein (1975, figure 7.2).

that the particle migrations were not limited by the presence of the walls was incorrect. We shall now examine this latter possibility in more detail.

The most extreme example of wall limitation occurs when the diffusion coefficient is sufficiently high that each observation of the position of the particle within the gap is uncorrelated with the previous one. Then if we were to continue to use (2.1) to calculate an observed value of the diffusion coefficient (the underlying assumption that the migrations are not limited by the walls of the device no longer being valid), we would obtain for an infinite diffusion coefficient

$$D_{\text{obs}}^{(\infty)} = \tfrac{1}{2}\langle \Delta y^2 \rangle \left\langle \frac{1}{\Delta t} \right\rangle, \tag{A 6}$$

where $\langle \Delta y^2 \rangle$ may be calculated from the probability distribution of observing the particle at a position y. Eckstein provides this distribution in figure 7.2 of his thesis (reproduced here as figure 7), which was for the same experimental conditions used to obtain the data given in figure 6. It is interesting to note that the distribution of particle observations given in figure 7 is very different from the linear profile expected from theory (2.23). This discrepancy suggests that the particle concentration near the walls of the Couette device was less than the average concentration across the gap. Although the mechanism leading to such a depletion in the wall regions (evidently more than could be accounted for by simple wall exclusion) is unclear, it is likely to be a result of the large particle diameter to gap width ratio used in this experiment, about 1:8. Since in our experimentation this ratio was less than 1:33, the wall-region depletion implied by figure 7 should have been much less significant.

In his data reduction procedure, Eckstein only counted migrations that originated in the central fifth of the Couette channel in an effort to minimize the effects of the wall. Recognizing this, we obtain

$$\langle \Delta y^2 \rangle = \int_0^W \int_{2W/5}^{3W/5} (y-y')^2 p(y) p'(y') \, \mathrm{d}y' \, \mathrm{d}y, \tag{A 7}$$

where $p(y)$ is the distribution given in figure 7 and $p'(y)$ is the probability distribution of particle observations that occur in the central fifth of the channel:

$$p'(y') = p(y') \Big/ \int_{2W/5}^{3W/5} p(y) \, \mathrm{d}y. \tag{A 8}$$

Integrating (A 7) numerically, we obtain $\langle \Delta y^2 \rangle \approx 0.29$ cm^2.

Given the estimated values of $\langle 1/\Delta t \rangle$ determined earlier, we may use (A 6) to

$\Delta t_{\min}$ (s)	4	10	20	30	40	50	60
D_{obs} (cm^2/s)	0.0162	0.0098	0.0057	0.0043	0.0035	0.0028	0.0028
D_{obs}^{∞} (cm^2/s)	0.0203	0.0109	0.0062	0.0043	0.0033	0.0027	0.0023

TABLE 2. Diffusion coefficients observed by Eckstein (1975) and those estimated for complete wall limitation by (A 6) as a function of $\Delta t_{\min}$.

compare the values of D_{obs} calculated by Eckstein (table 1) to those that would have been observed for an infinite diffusion coefficient. This is done in table 2 and, as may be seen, the assumption that the actual diffusion coefficient was infinite can account for the reported D_{obs}. The slight discrepancy between $D_{\text{obs}}^{(\infty)}$ and D_{obs} for small values of $\Delta t_{\min}$ indicates that the true diffusion coefficient, although perhaps much greater than the calculated value, was not infinite.

From the comparison given in table 2 it seems probable, therefore, that Eckstein's data were strongly influenced by the walls, at least for the particular experiment analysed here, the only experiment for which the data relevant to this analysis are available. Moreover, since Eckstein chose a value of $\Delta t_{\min} = 20$ s for the conditions $\dot{\gamma} = 10\ \text{s}^{-1}$, $a = \frac{1}{16}$ in. (the conditions of the experiment we have examined) and scaled his choice of $\Delta t_{\min}$ for all other experiments (denoted with a prime) such that

$$\Delta t'_{\min} = \Delta t_{\min} \frac{\dot{\gamma} a^2}{\dot{\gamma}' a'^2}, \tag{A 9}$$

it appears likely that all of his calculated diffusion coefficients were wall limited to a similar degree, at least for experiments where the concentration, and hence the diffusion coefficient, was large. At a sufficiently low concentration, however, we anticipate that the diffusion coefficient becomes small enough that the migrations are no longer wall limited. It is impossible to determine this point from Eckstein's data alone; however, from a comparison with the results of our experiments, it appears to occur at approximately 20%. Thus values of the diffusion coefficient observed by Eckstein (1975) at smaller concentrations are unlikely to have been influenced by wall effects.

REFERENCES

ECKSTEIN, E. C. 1975 Particle migration in a linear shear flow. Ph.D. thesis, Massachusetts Institute of Technology.

ECKSTEIN, E. C., BAILEY, D. G. & SHAPIRO, A. H. 1977 Self-diffusion of particles in shear flow of a suspension. *J. Fluid Mech.* **79**, 191.

FRANKEL, N. A. & ACRIVOS, A. 1968 Heat and mass transfer from small spheres and cylinders freely suspended in shear flow. *Phys. Fluids* **11**, 1913.

GRAHAM, A. L. & BIRD, R. B. 1984 Particle clusters in concentrated suspensions. 1. Experimental observations of particle clusters. *Ind. Engng Chem. Fundam.* **23**, 406.

GRAHAM, A. L. & STEELE, R. D. 1984 Particle clusters in concentrated suspensions. 2. Information theory and particle clusters. *Ind. Engng Chem. Fundam.* **23**, 411.

KARNIS, A., GOLDSMITH, H. L. & MASON, S. G. 1966 The kinetics of flowing dispersions. I. Concentrated suspensions of rigid particles. *J. Colloid Interface Sci.* **22**, 531.

LEIGHTON, D. & ACRIVOS, A. 1986 The shear induced migration of particles in concentrated suspensions. *J. Fluid Mech.* (submitted).

OKAGAWA, A., ENNIS, G. J. & MASON, S. G. 1978 Memory impairment in flowing suspensions. I. Some theoretical considerations. *Can. J. Chem.* **56**, 2815.